J. Phase Equilib. Diffus. (2021) 42:373–378
https://doi.org/10.1007/s11669-021-00888-8

An Updated Phase Diagram of the SnTe-Sb_2Te_3 System and the Crystal Structure of the New Compound $SnSb_4Te_7$

Aynur E. Seidzade[1,2] · Elnur N. Orujlu[1] · Thomas Doert[2] · Imamaddin R. Amiraslanov[4] · Ziya S. Aliev[3,4] · Mahammad B. Babanly[1]

Submitted: 5 December 2020 / in revised form: 22 March 2021 / Accepted: 30 April 2021 / Published online: 1 June 2021

Abstract The phase equilibria in the SnTe-Sb_2Te_3 system were re-investigated by a combination of Differential Thermal Analysis (DTA), Powder x-ray Diffraction (PXRD), and Scanning Electron Microscope equipped with Energy Dispersive x-ray Spectrometer (SEM-EDS) techniques. In an earlier reported version, this phase diagram was described as quasi-binary with only one intermediate compound, namely $SnSb_2Te_4$. Here we report the existence of the new van der Waals type compound $SnSb_4Te_7$ for the first time. Considerable homogeneity ranges for both ternary compounds are also revealed. According to DTA results, peritectic melting was found for both compounds. The corresponding temperatures were found to be 595 and 593 °C for $SnSb_2Te_4$ and $SnSb_4Te_7$, respectively. The PXRD pattern of the newly found phase was analyzed through the Rietveld method and the crystal structure was solved. In the considered quasi-binary system, two wide solid-solubility areas based on the constitutive compounds were also revealed.

Keywords crystal structure · phase diagram · SnTe-sb_2te_3 system · solid solutions · topological insulators · van der waals compound

✉ Ziya S. Aliev
ziyasaliev@gmail.com

[1] Institute of Catalysis and Inorganic Chemistry of ANAS, AZ1143 Baku, Azerbaijan

[2] Technical University of Dresden, Helmholtz str. 10, 01069 Dresden, Germany

[3] Azerbaijan State Oil and Industry University, AZ1010 Baku, Azerbaijan

[4] Institute of Physics of ANAS, AZ1143 Baku, Azerbaijan

1 Introduction

During the last forty years, chalcogenide-based layered materials have been widely studied due to their promising electro-physical properties. Particularly, tetradymite-type (mixed) layered ternary phases of the quasi-binary $A^{IV}Te$-$A^{V}{}_2Te_3$ (A^{IV} = Ge, Sn; A^{V} = Sb, Bi) systems exhibit good electrical and significant low thermal conductivity which are key aspects for promising thermoelectric materials [1–3]. Thus, these materials are expected to have potential applications in the fabrication of high-performance solid-state coolers and waste heat recovery from different energy sources [4–7]. Since 2010, the $nA^{IV}Te{\bullet}mA^{V}{}_2Te_3$ homologous series of phases have been confirmed experimentally and theoretically as 3D topological insulator phases of quantum matter [8–11]. Thus, the unique properties of these ternaries make them tunable materials that exhibit both topological insulating and good thermoelectric properties [12–14]. Given the growing interest in this class of tunable materials, the re-investigation of one of the above-mentioned quasi-binary systems—the SnTe-Sb_2Te_3 phase diagram, is of particular importance for the chemical design of its intermediate phases.

In a previous report, the phase diagram of the SnTe-Sb_2Te_3 was found to host only one intermediate compound, namely $SnSb_2Te_4$, which has a wide homogeneity range [15, 16] and melts incongruently at 603 °C [16]. The tetradymite-type hexagonal crystal structure and lattice parameters of $SnSb_2Te_4$ (R-3m, a = 4.298(1) Å, c = 41.57(1) Å) were determined by using resonant single-crystal diffraction later [17]. A so-called 21R-type structure consisting of septuple rocksalt-type blocks are weakly connected by van der Waals (vdW) interactions. Each septuple block consists of four anion and three cation layers. Although tin atoms are distributed over all cation

positions, most of them were found clustered in the central layers of the septuple blocks.

The Gibbs free energy and enthalpy, as well as the electronic structure and dynamics at the surface of the $SnSb_2Te_4$, were given in our previous works [18, 19].

The existence of the $SnSb_4Te_7$ is mentioned in Refs. [20, 21] where its crystal structure was determined by electron diffraction from thin-films: *P*-3*m*1, a = 4.37 Å; c = 23.78 Å [20]. An electronic and spin structure of this compound is theoretically calculated in [21]. However, polycrystalline $SnSb_4Te_7$ was successfully synthesized in our recent work [22] for the first time.

Here we provide new results, which require a revision of the SnTe-Sb_2Te_3 phase diagram, including the new compound $SnSb_4Te_7$ and its crystal structure.

2 Experimental Part

Both the starting compounds of the title system were synthesized by melting of high purity elements (99.999 wt.% Alfa Aesar) in evacuated ($\sim 10^{-3}$ Pa) silica ampoules at temperatures ~50 °C higher than their melting points. The constitution of the synthesized compounds was checked by means of DTA and PXRD techniques.

Totally seventeen alloys from the examined system (alloy compositions are shown as black circles in Fig. 5) were prepared by melting of the pre-synthesized starting compounds in various ratios approximately at 800 °C followed by water-quenching. The alloys were further annealed at 450 °C for 720 h to achieve equilibrium state.

Bulk single-crystalline ingots of the various alloys of the system with 3.5 cm in length and 0.8 cm in diameter were grown by the vertical Bridgman-Stockbarger method. In the growth process, the charged ampoules were held in the "hot" zone (~650 °C) of the furnace for 6h and then were moved to the "cold" zone of the furnace with a rate of 1.0 mm/h.

PXRD data collection was performed at room temperature with Bruker D2 Phaser diffractometer and with an Empyrean diffractometer (PANalytical) equipped with a curved Ge(111) monochromator. In both measurements, the CuKα_1 radiation was used as x-ray source. Rietveld refinement using the fundamental parameter approach was performed with TOPAS 4.2 academic software. Morphological characterizations of the samples were done with SU8020 Scanning Electron Microscope (Hitachi) equipped with a triple detector system (U_a = 5 kV). DTA of the annealed alloys was carried out using SETARAM Instrumentation system (temperature accuracy ±2 °C) from room temperature up to 1000 °C with a heating and cooling rate of 5 °C·min^{-1}. Temperatures of thermal effects were taken mainly from the heating curves.

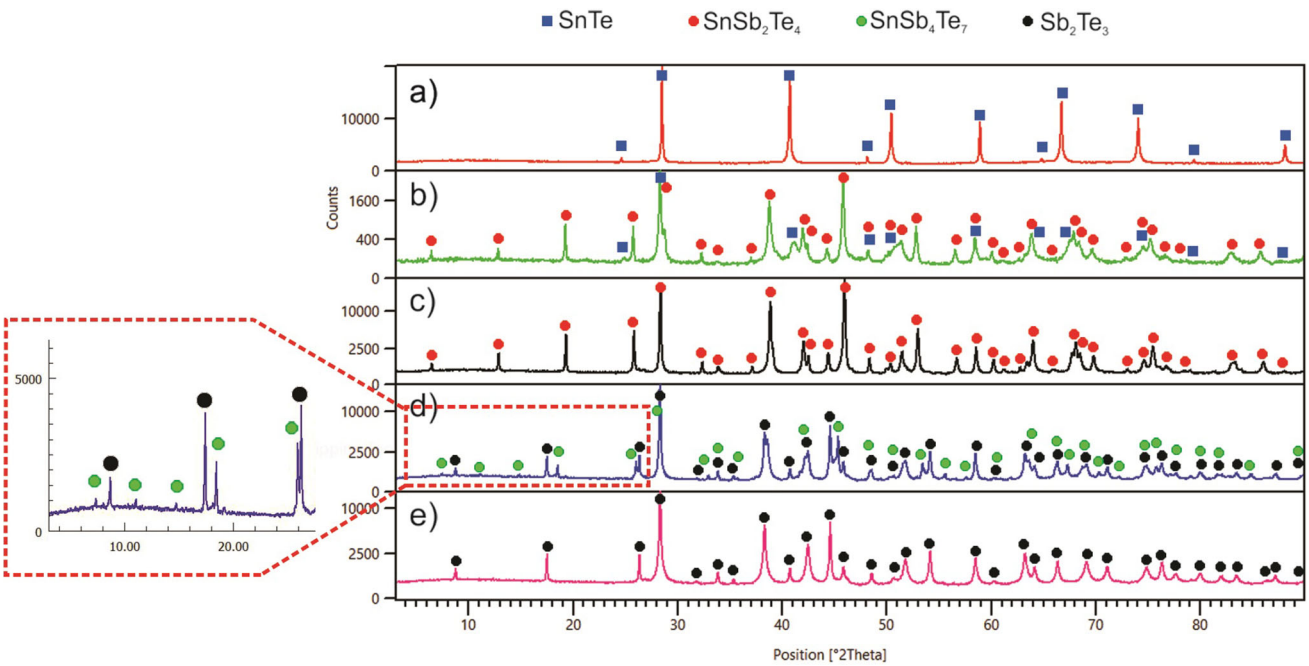

Fig. 1 PXRD patterns of the SnTe-Sb2Te3 alloys: (a), 10 mol.% Sb2Te3; (b), 40 mol.% Sb2Te3; (c), 50 mol.% Sb2Te3; (d), 75 mol.% Sb2Te3; (e), 85 mol.% Sb2Te3

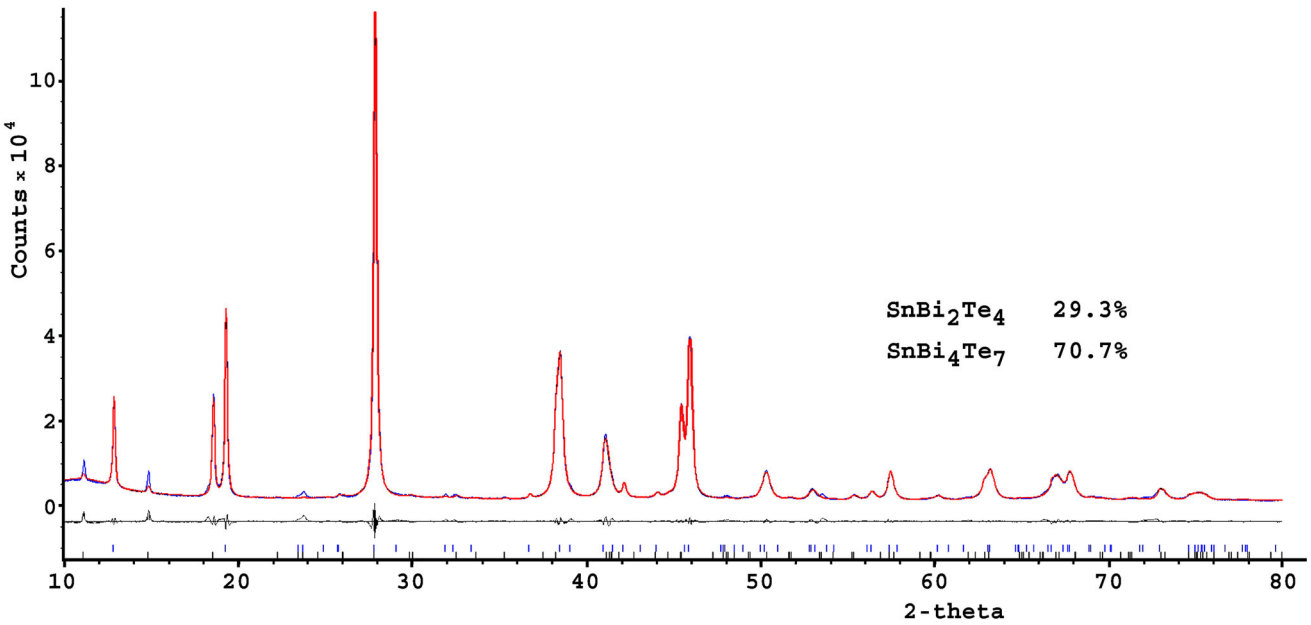

Fig. 2 Rietveld refinement of the diffraction pattern of the alloy containing 60 mol.% Sb2Te3

Table 1 Refined crystal structure data for the SnSb4Te7 phase

Compound	$SnSb_4Te_7$
R-Bragg	1.212
Space group	*P*-3*m*1
Lattice parameters	
a, Å	4.2951(2)
c, Å	23.973(8)
Unit cell volume, $Å^3$	383.00(2)
Crystal density, g/cm^3	6.228(3)

Table 2 Experimentally determined atomic coordinates, cation-anion band distances and their multiplicity (in brackets) for the SnSb4Te7.

Atom	Position	*x/a*	*y/b*	*z/c*	B_{eq}, nm^2 x10^2
Sn	1a	0	0	0	1
Te(1)	2d	2/3	1/3	0.0788(8)	1
Sb(1)	2d	1/3	2/3	0.1657(7)	1
Te(2)	2c	0	0	0.2507(11)	1
Te(3)	2d	2/3	1/3	0.3572(11)	1
Sb(2)	2d	1/3	2/3	0.4125(7)	1
Te(4)	1b	0	0	0.5	1
Atoms					Distances, Å
Sn—Te					3.146 (x6)
Sb(1)—Te(1); Te(2)					3.295 (x3); 3.250 (x3)
Sb(2)—Te(3); Te(4)					2.858 (x3); 3.289 (x3)

Please note that possible atomic disorder was not considered in the Rietveld refinements

3 Results and Discussion

In order to re-study the phase equilibria in the SnTe-Sb_2Te_3 system, seventeen samples were synthesized with different SnTe:Sb_2Te_3 starting ratios. The PXRD patterns of five of these samples are given in Fig 1. As can be seen from Fig. 1a and e, the PXRD results of the SnTe- and Sb_2Te_3-rich samples have qualitatively identical diffraction pattern showing pure tin and antimony tellurides, respectively. The intermediate samples having 10 mol.% (Fig. 1a) and 85 mol.% Sb_2Te_3 (Fig. 1e) exhibit similar diffraction lines with a negligible shifting compared to pure SnTe and Sb_2Te_3, respectively. The results obviously confirm the existence of a solid solubility field based on SnTe (α phase, ~11–12 mol.%) and based on Sb_2Te_3 (β phase, ~20 mol.%). The sample containing 40 mol.% Sb_2Te_3 was found to be a biphasic mixture of α-SnTe and $SnSb_2Te_4$ (Fig. 1b), while the sample having 50 mol.% Sb_2Te_3 which is corresponding to ternary compound $SnSb_2Te_4$, is phase-pure (Fig. 1c). The sample having 66.7 mol.% Sb_2Te_3 (nominally $SnSb_4Te_7$) was a mixture of several phases. These results indicate, that the samples did not reach the thermodynamic equilibrium despite long-time thermal annealing. However, both ternary compounds can easily be distinguished in PXRD analysis by their typical diffraction peaks, particularly at small angles. The 75 mol.% Sb_2Te_3 sample shows reflections of Sb_2Te_3 and $SnSb_4Te_7$ which do not match those of other possible phases (Fig. 1d).

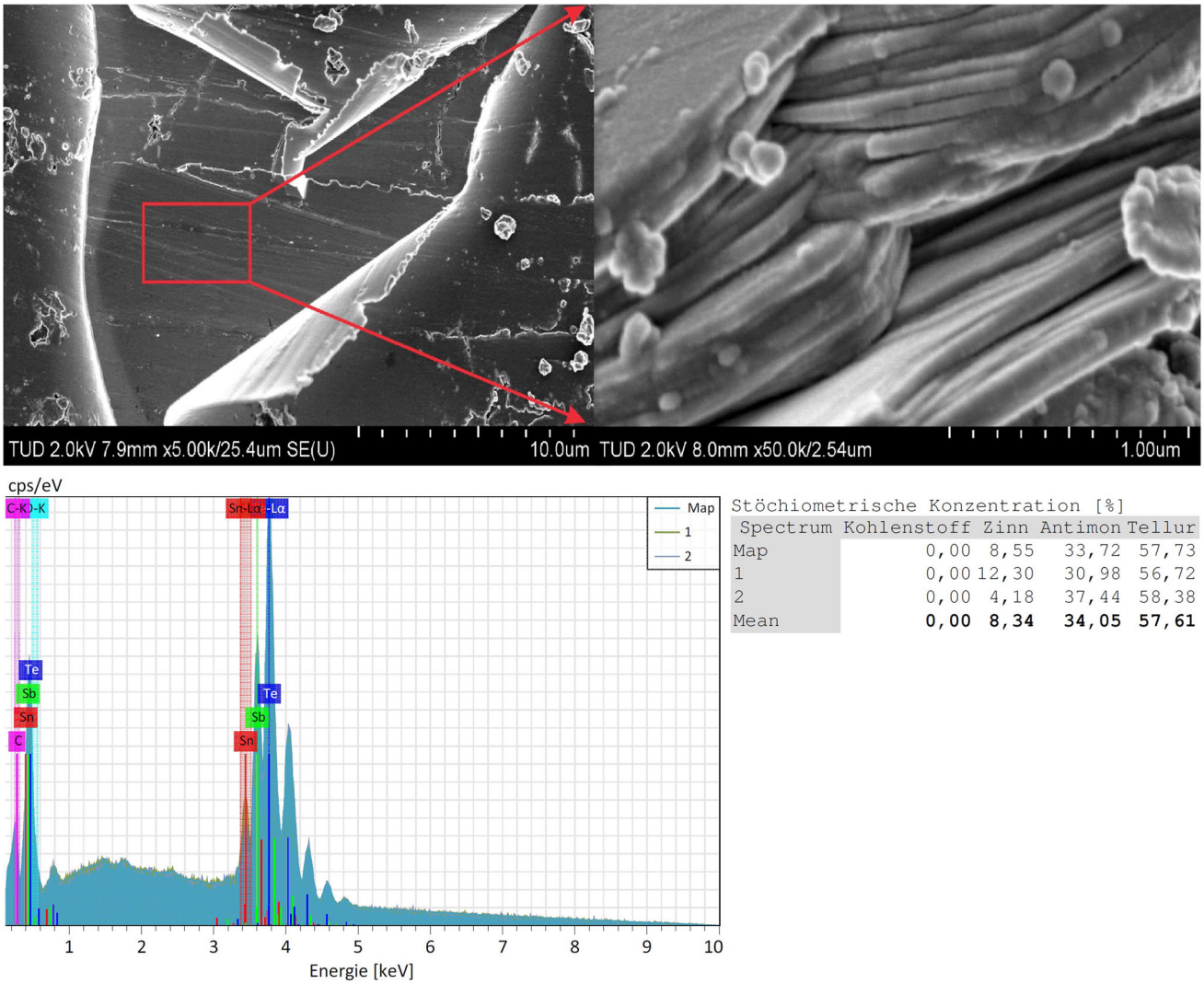

Fig. 3 The SEM micrograph, EDS spectrum and EDS elemental microanalysis data for the selected area of the alloy having 75 mol.% Sb2Te3

Hence, these PXRD results confirm the formation of the new $SnSb_4Te_7$ compound in the SnTe-Sb_2Te_3 system.

The analysis of the samples obtained through the Bridgman-Stockbarger method confirms the existence of the newly revealed $SnSb_4Te_7$ as well. PXRD analysis of the single crystalline sample taken from the upper part of the as-grown ingot having 60 mol.% Sb_2Te_3 shows that it exhibits diffraction lines according to both $SnSb_4Te_7$ and $SnSb_2Te_4$ (Fig. 2). We did not detect typical diffraction intensities for higher members of the $n(SnTe)\bullet m(Sb_2Te_3)$ (n=1, m>2) homologous series which are formed in the analogous system SnTe-Bi_2Te_3. The existence of large homogeneity fields based on both starting binary tellurides indicates that tin and antimony can replace each other to a certain extend on the cation sites of the crystal lattice. Such a mutual replacement of Sn and Sb atoms may also occur in the septuple and septuple-quintuple blocks of the $SnSb_2Te_4$ and $SnSb_4Te_7$ ternary compounds, respectively. This kind of cation intermixing and similar atomic sizes of the Sn and Sb atoms are probably the main reasons that prevent the formation of the higher homologues and, thus, more complex layered structures than $SnSb_4Te_7$.

To reveal the crystal structure of the newly synthesized $SnSb_4Te_7$, the PXRD pattern of the sample with 60 mol.% Sb_2Te_3 was refined by the Rietveld method (Fig. 2). The Rietveld refinement was performed on this alloy since no phase-pure sample of this compound could be obtained under the applied experimental conditions. Details of the crystal structure refinement and atomic parameters are summarized in Tables 1 and 2. An analysis of the XRD pattern shows that along with $SnSb_2Te_4$ (∼29.3%), the sample contains $SnSb_4Te_7$ as second phase which is indexed in the trigonal crystal system with the unit cell parameters a=4.2951(2) Å and c=23.973(8) Å. From the reflection conditions, space group P-3m1 was assumed for $SnSb_4Te_7$. The Rietveld fitted pattern (Fig. 2) shows that

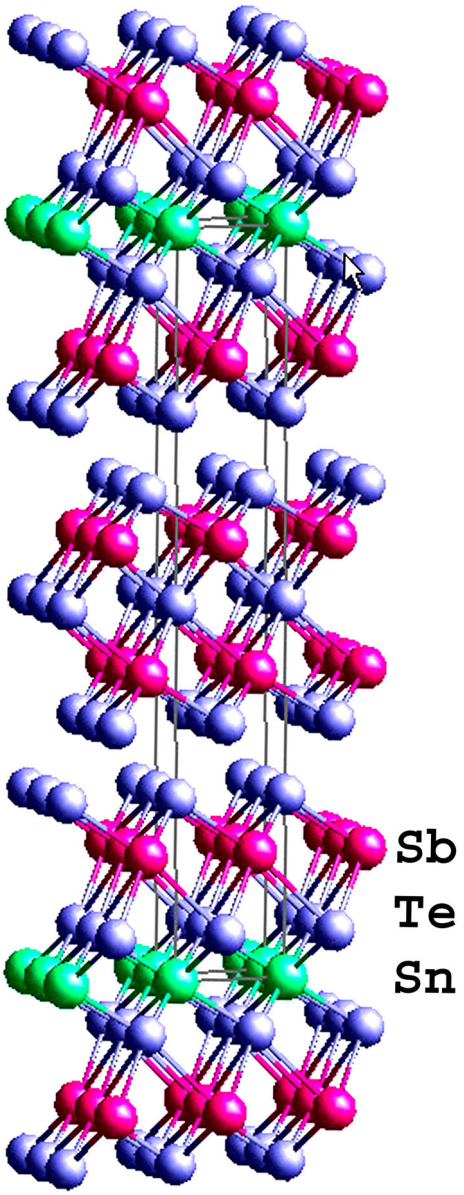

Fig. 4 Visualized crystal structure projection of the SnSb4Te7

the dominant phase in this sample is the $SnSb_4Te_7$ (~70%). SEM-EDS measurements further confirm the existence of the $SnSb_4Te_7$ phase in this sample. Fig. 3 summarizes the SEM micrograph, EDS spectrum, and EDS elemental microanalysis results for the selected area of the 60 mol.% Sb_2Te_3 sample where $SnSb_4Te_7$ is the majority phase.

The crystal structure of $SnSb_4Te_7$ is shown in Fig 4. As can be seen, the structure is an alternation of quintuple (five-layer) Te-Bi-Te-Bi-Te and septuple (seven-layer) Te-Bi-Te-Sn-Te-Bi-Te blocks along the c-axes. The first building block resembles the crystal structure of Sb_2Te_3, whereas the latter is the repeat unit of the crystal structure of $SnSb_2Te_4$ (17). Interatomic bonds within both building

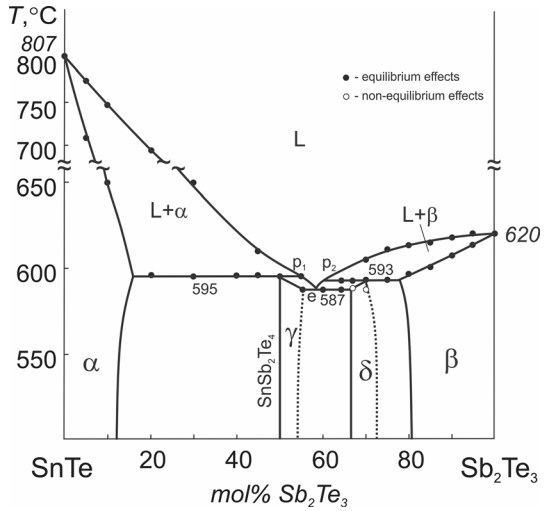

Fig. 5 An updated phase diagram of the SnTe-Sb2Te3 quasi-binary system

blocks can be considered as covalent, whereas the interaction between the two neighbor blocks is of a weak van der Waals type.

Thereby, the newly synthesized $SnSb_4Te_7$ is the structural analogous of tetradymite-derivative mixed-layered $A^{IV}A^{V}{}_4Te_7$ compounds, which were earlier reported in most of the $A^{IV}Te$-$A^{V}{}_2Te_3$ systems, where A^{IV} = Ge, Sn, Pb and A^{V} = Sb, Bi.

Because the novel $SnSb_4Te_7$ compound has been found in the SnTe-Sb_2Te_3 system, the phase diagram was re-plotted based on experimental data from DTA and XRD analysis of the equilibrated alloys (Fig. 5). The system is found to be a quasi-binary one and features the formation of the two intermediate compounds by the following peritectic reactions:

$$L + a(SnTe) \leftrightarrow SnSb_2Te_4(p_1, 595\,^{\circ}C)$$
$$L + b(Sb_2Te_3) \leftrightarrow SnSb_4Te_7(p_2, 593^{\circ}C)$$

Along the system, the coordinates of the peritectic p_1 and p_2 points were found to be at 53 mol.% and 59 mol.% Sb_2Te_3, respectively. The temperature of eutectic transformation was measured as 587 °C at 58 mol.% Sb_2Te_3. As can be seen from Fig. 5, the $SnSb_4Te_7$ has a very narrow primary crystallization area meaning that it is extremely difficult to obtain a phase-pure crystalline sample via direct solidification. The primary experimental data show that $SnSb_4Te_7$ has a significant homogeneity area (δ phase) approximately from 66.5 to 72.7 mol.% Sb_2Te_3. Similar size of the homogeneity field for $SnSb_2Te_4$ (γ phase) has also been detected approximately from 50 to 54 mol.% Sb_2Te_3. Besides, the system has two more homogeneity areas based on both initial SnTe (α phase, up to ~11-13 mol.% at room temperature) and Sb_2Te_3 (β phase, up to ~18-19 mol.% at room temperature) compounds. It is

worth mentioning that the updated phase diagram for the SnTe-Sb_2Te_3 systems differs from the earlier known version (14, 15) in terms of the number of ternary compounds, as well as for peritectic and eutectic reaction temperatures. This might have been overlooked previously as the two peritectic temperatures are very close to each other and the reflections, which allow for an unambiguous identification of the new compound $SnSb_4Te_7$ are of comparatively low intensity.

4 Conclusion

New experimental data on the phase equilibria of the SnTe-Sb_2Te_3 system were obtained by means of DTA, PXRD, and SEM-EDS analyses which are significantly different from earlier reported ones. An updated phase diagram is featured by the formation of the two ternary $SnSb_2Te_4$ and $SnSb_4Te_7$ compounds that melt peritectically at 595 °C and 593 °C, respectively. The primary crystallization fields for both ternary phases as well as types and coordinates of nonvariant equilibria were determined. The existence of homogeneity areas based on both ternary compounds and the initial phases SnTe and Sb_2Te_3 was detected. The crystal structure of the newly synthesized $SnSb_4Te_7$ was solved by Rietveld refinement. An updated phase diagram of the SnTe-Sb_2Te_3 system provides very valuable information for designing the synthesis and single crystal growth experiments of multifunctional ternary materials.

Acknowledgment The work was partially supported by the Science Development Foundation under the President of the Republic of Azerbaijan, a grant EİF/MQM/Elm-Tehsil-1-2016-1(26)-71/01/4-M-33 and by the DAAD program (Deutscher Akademischer Austauschdienst) as part of the Research Grants: Bi-nationally Supervised Doctoral Degree". Special thanks to the Markus Schmidt, Max Planck Institute of Chemical Physics of Solids for cooperation in crystal growth by the Bridgman technique.

References

1. L.E. Shelimova, O.G. Karpinskii, P.P. Konstantinov, E.S. Avilov, M.A. Kretova, and V.A. Zemskov, Crystal Structures and Thermoelectric Properties of Layered Compounds in the ATe-Bi_2Te_3 (A=Ge, Sn, Pb) Systems, *Inorg. Mater.*, 2004, **40**(5), p 530–540
2. F. von Rohr, A. Schilling, and R.J. Cava, Single-crystal Growth, and Thermoelectric Properties of Ge(Bi, Sb)4Te7, *J. Phys. Condens. Matter.*, 2013, **25**(7), p 075804
3. D. Wu, L. Xie, X. Xu, and J.Q. He, High Thermoelectric Performance Achieved in GeTe—Bi_2Te_3 Pseudo-Binary via Van der Waals Gap-Induced Hierarchical Ferroelectric Domain Structure, *Adv. Funct. Mater.*, 2019, **29**(18), p 1806613
4. G.K. Ahluwalia, *Applications of Chalcogenides: S, Se, and Te*. Springer, Cham, 2016.
5. D.L. Duong, S.J. Yun, and Y.H. Lee, van der Waals Layered Materials: Opportunities and Challenges, *ACS Nano*, 2017, **11**(12), p 11803–11830
6. J. He, and T.M. Tritt, Advances in Thermoelectric Materials Research: Looking Back and Moving Forward, *Science*, 2017, **357**(6358), p 9997
7. Z. Tiejun, Y. Liu, C. Fu, J.P. Heremans, J.G. Snyder, and X. Zhao, Compromise and Synergy in High-efficiency Thermoelectric Materials, *Adv. Mater.*, 2017, **29**, p 1605884
8. L.L. Wang, and D.D. Johnson, Ternary Tetradymite Compounds as Topological Insulators, *Phys. Rev. B*, 2011, **83**(24), p 241309
9. M.B. Babanly, E.V. Chulkov, Z.S. Aliev, A.V. Shevelkov, and I.R. Amiraslanov, Phase Diagrams in the Materials Science of Topological Insulators Based on Metal Chalcogenides, *Russ. J. Inorg. Chem.*, 2017, **62**(13), p 1703–1729
10. M. Nurmamat, K. Okamoto, S. Zhu, T.V. Menshchikova, I.P. Rusinov, V.O. Korostelev, K. Miyamoto, T. Okuda, T. Miyashita, X. Wang, Y. Ishida, K. Sumida, E.F. Schwier, M. Ye, Z.S. Aliev, M.B. Babanly, I.R. Amiraslanov, E.V. Chulkov, K.A. Kokh, O.E. Tereshchenko, K. Shimada, S. Shin, and A. Kimura, Topologically Non-trivial Phase-change Compound $GeSb_2Te_4$, *ACS Nano*, 2020, **14**(7), p 9059–9065
11. D. Pacile, S.V. Eremeev, M. Caputo, M. Pisarra, O. De Luca, I. Grimaldi, J. Fujii, Z.S. Aliev, M.B. Babanly, I. Vobornik, R.G. Agostino, A. Goldoni, E.V. Chulkov, and M. Papagno, Deep Insight into the Electronic Structure of Ternary Topological Insulators: A Comparative Study of $PbBi_4Te_7$ and $PbBi_6Te_{10}$, *Phys. Status Solidi*, 2018, **12**(12), p 1800341–1800348
12. J.P. Heremans, R.J. Cava, and N. Samarth, Tetradymites as Thermoelectrics and Topological Insulators, *Nat. Rev. Mater.*, 2017, **2**(10), p 17049
13. N. Xu, Y. Xu, and J. Zhu, Topological Insulators for Thermoelectrics, *npj Quant. Mater.*, 2017, **2**, p 51
14. D. Baldomir, and D. Faílde, On Behind the Physics of the Thermoelectricity of Topological Insulators, *Sci. Rep.*, 2019, **9**, p 6324
15. A. Stegherr, Das dreistoffsystem zinn-antimon-tellur, *Philips Res. Rep.*, 1969, **6**, p 1–71, **in German**
16. E.I. Elagina, and N.K. Abrikosov, The Investigation of the Systems PbTe–Bi_2Te_3 and SnTe–Sb_2Te_3, *Russ. J. Inorg. Chem.*, 1959, **4**, p 1638–1642
17. O. Oeckler, M.N. Schneider, F. Fahrnbauer, and G. Vaughan, Atom Distribution in $SnSb_2Te_4$ by Resonant x-ray Diffraction, *Solid State Sci.*, 2011, **13**, p 1057–1161
18. F.N. Guseinov, A.E. Seidzade, Y.A. Yusibov, and M.B. Babanly, Thermodynamic Properties of the $SnSb_2Te_4$ Compound, *Inorg. Mater.*, 2017, **53**(4), p 354–357
19. D. Niesner, S. Otto, V. Hermann, T. Fauster, T.V. Menshchikova, S.V. Eremeev, Z.S. Aliev, I.R. Amiraslanov, M.B. Babanly, P.M. Echenique, and E.V. Chulkov, Bulk and Surface Electron Dynamics in a p-type Topological Insulator $SnSb_2Te_4$, *Phys. Rev. B*, 2014, **89**, p 081404
20. R.M. Imamov, S.A. Semiletov, and Z.G. Pinsker, The Crystal Chemistry of Semiconductors with Octradral and with Mixed Atomic Coordination, *Kristallografiya*, 1970, **15**, p 239–243
21. M.G. Vergniory, T.V. Menshchikova, I.V. Silkin, Y.M. Koroteev, S.V. Eremeev, and E.V. Chulkov, Electronic and Spin Structure of a Family of Sn-based Ternary Topological Insulators, *Phys. Rev. B*, 2015, **92**(4), p 045134
22. A.E. Seidzade, Phase Diagram of the $SnSb_4Te_7$-$SnBi_4Te_7$ System, *New Mater. Compd. Appl.*, 2019, **3**(3), p 193–197